Supplement of Atmos. Chem. Phys., 15, 4161–4178, 2015
http://www.atmos-chem-phys.net/15/4161/2015/
doi:10.5194/acp-15-4161-2015-supplement

Atmospheric Chemistry and Physics Open Access

Supplement of

Single-particle characterization of ice-nucleating particles and ice particle residuals sampled by three different techniques

A. Worringen et al.

Correspondence to: S. Weinbruch (weinbruch@geo.tu-darmstadt.de)

Table S1: sampling times and operating conditions for the FINCH+IN-PCVI / SEM impactor coupling

sampling day	sampling time, UTC	mean temperature, °C	temperature standard deviation, °C	mean saturation ratio with respect to ice	standard deviation of the saturation ratio
Feb. 2, 2013	14:50 – 17:11	-22.0	0.5	1.72	0.18
Feb. 4, 2013	06:16 – 08:27	-23.3	1.1	1.70	0.08
Feb. 4, 2013	12:00 – 14:51	-21.1	1.2	1.80	0.06
Feb. 5, 2013	17:45 – 20:15	-19.9	1.0	1.72	0.15
Feb. 6, 2013	15:47 – 21:05	-21.3	2.0	1.35	0.07
Feb. 7, 2013	08:05 – 11:32	-19.6	0.9	1.40	0.18
Feb. 8, 2013	18:23 – 22:52	-22.8	0.3	1.20	0.03
Feb. 9, 2013	17:08 – 22:39	-22.2	0.7	1.14	0.08
Feb. 10, 2013	10:00 – 13:41	-22.9	0.7	1.31	0.06
Feb. 10, 2013	17:34 – 21:20	-21.8	1.2	1.70	0.06
Feb. 11, 2013	08:08 – 13:26	-21.8	1.5	1.50	0.11
Feb. 13, 2013	14:02 – 15:30	-24.9	0.4	1.61	0.18
Feb. 14, 2013	08:41 – 13:01	-25.1	1.2	1.49	0.11
Feb. 17, 2013	08:54 – 12:36	-23.4	0.4	1.50	0.13
Feb. 19, 2013	08:47 – 12:59	-20.8	1.8	1.66	0.17
Feb. 20, 2013	08:37 – 11:58	-21.2	1.1	1.66	0.06
Feb. 21, 2013	08:35 – 14:18	-21.9	1.4	1.65	0.11
Feb. 22, 2013	06:09 – 13:49	-21.7	1.2	1.57	0.07

Table S2: Relative number abundance [%] integrated over all samples of different particle groups as function of sampling technique and for a particle size < 1 µm. Also given are 95 % confidence intervals [%]. The data are displayed in Fig. 4 of the publication.

	ISI (n = 91)		FINCH + IN-PCVI (n = 902)		Ice-CVI (n = 962)	
d < 1 µm	**Rel. abund.**	**95 % CI**	**Rel. abund.**	**95 % CI**	**Rel. abund.**	**95 % CI**
Carbonaceous	39.6	29.5 – 50.4	5.1	3.8 – 6.7	3.8	2.7 – 5.3
Carbonaceous + inclusion	2.2	0.3 – 7.7	5.7	4.2 – 7.4	1.1	0.6 – 2.0
Secondary	5.5	1.8 – 12.4	0.4	0.1 – 1.1	0.6	0.2 – 1.4
Sulfate	9.9	4.6 – 17.9	21.2	18.6 – 24.0	5.1	3.8 – 6.7
Sulfate + inclusion	0.0	0.0 – 4.0	0.3	0.1 – 1.0	0.1	0.0 – 0.6
Soot	2.2	0.3 – 7.7	2.1	1.3 – 3.3	2.9	1.9 – 4.2
Soot mixture	1.1	0.0 – 6.0	0.1	0.0 – 0.6	0.2	0.0 – 0.7
Sea-salt	2.2	0.3 – 7.7	0.2	0.0 – 0.8	6.9	5.3 – 8.6
Sea-salt + inclusion	0.0	0.0 – 4.0	0.2	0.0 – 0.8	0.5	0.2 – 1.2
Ca-rich	2.2	0.3 – 7.7	3.3	2.3 – 4.7	2.2	1.4 – 3.3
Ca-rich + inclusion	0.0	0.0 – 4.0	0.3	0.1 – 1.0	0.1	0.0 – 0.6
Metal oxide	17.6	10.4 – 27.0	4.9	3.6 – 6.5	4.2	3.0 – 5.6
Metal oxide + coating	0.0	0.0 – 4.0	6.1	4.6 – 7.9	2.1	1.3 – 3.2
Silicate	6.6	2.5 – 13.8	11.2	9.2 – 13.4	35.9	32.8 – 39.0
Silicate mixture	4.4	1.2 – 10.9	18.1	15.6 – 20.7	20.1	17.6 – 22.7
Pb-bearing	0.0	0.0 – 4.0	0.3	0.1 – 1.0	9.6	7.8 – 11.6
Droplet	4.4	1.2 – 10.9	17.2	14.8 – 19.8	3.6	2.5 – 5.0
Other	2.2	0.3 – 7.7	3.2	2.2 – 4.6	1.0	0.5 – 1.9

Table S3: Relative number abundance [%] integrated over all samples of different particle groups as function of sampling technique and for a particle size > 1 µm. Also given are 95 % confidence intervals [%]. The data are displayed in Fig. 4 of the publication.

	ISI (n = 105)		FINCH + IN-PCVI (n = 456)		Ice-CVI (n = 111)	
d > 1 µm	**Rel. abund.**	**95 % CI**	**Rel. abund.**	**95 % CI**	**Rel. abund.**	**95 % CI**
Carbonaceous	17.1	10.5 – 25.7	2.4	1.2 – 4.3	0.9	0.0 – 4.9
Carbonaceous + inclusion	1.9	0.2 – 6.7	11.0	8.2 – 14.2	3.6	1.0 – 9.0
Secondary	2.9	0.6 – 8.1	0.9	0.2 – 2.2	0.0	0.0 – 3.3
Sulfate	0.0	0.0 – 3.5	1.3	0.5 – 2.8	0.0	0.0 – 3.3
Sulfate + inclusion	0.0	0.0 – 3.5	0.2	0.0 – 1.2	0.9	0.0 – 4.9
Soot	3.8	1.0 – 9.5	0.0	0.0 – 0.8	0.0	0.0 – 3.3
Soot mixture	0.0	0.0 – 3.5	0.0	0.0 – 0.8	0.0	0.0 – 3.3
Sea-salt	2.9	0.6 – 8.1	0.9	0.2 – 2.2	11.7	6.4 – 19.2
Sea-salt + inclusion	1.0	0.0 – 5.2	1.1	0.4 – 2.5	2.7	0.6 – 7.7
Ca-rich	14.3	8.2 – 22.5	12.3	9.4 – 15.6	3.6	1.0 – 9.0
Ca-rich + inclusion	1.9	0.2 – 6.7	0.9	0.2 – 2.2	0.9	0.0 – 4.9
Metal oxide	5.7	2.1 – 12.0	0.9	0.2 – 2.2	0.0	0.0 – 3.3
Metal oxide + coating	0.0	0.0 – 3.5	9.0	6.5 – 12.4	4.5	1.5 – 10.2
Silicate	10.5	5.3 – 18.0	18.0	14.5 – 21.8	19.8	12.9 – 28.5
Silicate mixture	21.0	13.6 – 30.0	28.3	24.2 – 32.7	18.0	11.4 – 26.4
Pb-bearing	0.0	0.0 – 3.5	1.5	0.6 – 3.1	22.5	15.1 – 31.4
Droplet	15.2	9.0 – 23.6	8.1	5.8 – 11.0	10.8	5.7 – 18.1
Other	1.9	0.2 – 6.7	3.3	1.9 – 5.4	0.0	0.0 – 3.3

Table S4: Relative number abundance [%] of different particle groups among INP/IPR for 2 February determined by Ice-CVI and FINCH + IN-PCVI. Also given are 95 % confidence intervals [%]. The data are displayed in Fig. 5 of the publication.

	Ice-CVI (n = 395)		FINCH+ IN-PCVI (n = 28)	
	Rel. abund.	**95 % CI**	**Rel. abund.**	**95 % CI**
Carbonaceous	2.3	1.0 – 4.3	7.1	0.9 – 23.5
Carbonaceous + inclusion	1.8	0.7 – 3.6	7.1	0.9 – 23.5
Secondary	0.3	0.0 – 1.4	0.0	0.0 – 12.3
Sulfate	0.8	0.2 – 2.2	0.0	0.0 – 12.3
Sulfate + inclusion	0.0	0.0 – 0.9	0.0	0.0 – 12.3
Soot	0.5	0.1 – 1.8	0.0	0.0 – 12.3
Soot mixture	0.3	0.0 – 1.4	0.0	0.0 – 12.3
Sea-salt	1.5	0.6 – 3.3	0.0	0.0 – 12.3
Sea-salt + inclusion	0.5	0.1 – 1.8	0.0	0.0 – 12.3
Ca-rich	1.5	0.6 – 3.3	0.0	0.0 – 12.3
Ca-rich + inclusion	0.0	0.0 – 0.9	0.0	0.0 – 12.3
Metal oxide	2.3	1.0 – 4.3	10.7	2.3 – 28.2
Metal oxide + coating	2.8	1.4 – 4.9	3.6	0.1 – 18.3
Silicate	45.3	40.3 – 50.4	57.1	37.2 – 75.6
Silicate mixture	26.6	22.3 – 31.2	10.7	2.3 – 28.2
Pb-bearing	11.4	8.4 – 14.9	0.0	0.0 – 12.3
Droplet	1.8	0.7 – 3.6	3.6	0.1 – 18.3
Other	0.5	0.1 – 1.8	0.0	0.0 – 12.3

Table S5: Comparison of the composition/mixing state of Pb-bearing particles from INUIT (present contribution) and CLACE 5 (Ebert et al., 2011) from the Ice-CVI. Also given are 95 % confidence intervals [%]. The data are displayed in Fig. 9 of the publication.

	INUIT (n = 118)		CLACE 5 (n = 575)	
	Rel. abund.	**95 % CI**	**Rel. abund.**	**95 % CI**
C-O-(S)-bearing	8.5	4.1 – 15.0	11.0	8.5 – 13.8
Soot	0.8	0.0 – 4.6	0.0	0.0 – 0.6
Sea-salt / sulfate	26.3	18.6 – 35.2	19.0	15.8 – 22.4
Ca-rich	5.1	1.9 – 10.7	3.0	1.7 – 4.7
Al-rich	11.9	6.6 – 19.1	4.0	2.6 – 5.9
Metal oxides	0.0	0.0 – 3.1	1.0	0.4 – 2.3
Silicates	27.1	19.3 – 36.1	32.0	28.2 – 36.0
Homogeneous Pb-rich	5.1	1.9 – 10.7	13.0	10.4 – 16.1
Other	15.3	9.3 – 23.0	17.0	14.1 – 20.4

Table S6: Comparison of particle class relative number abundance [%] determined by SEM-EDX and LA-MS for IPR sampled by ISI and Ice-CVI. Also given are 95 % confidence intervals [%]. The data are displayed in Fig. 10 of the publication.

	ISI		Ice–CVI	
	Rel. abund.	**95 % CI**	**Rel. abund.**	**95 % CI**
SEM–EDX	(n = 196)		(n = 1073)	
Carbonaceous + soot	35.9	29.2 – 43.0	7.8	6.3 – 9.6
Pb-rich	0.0	0.0 – 1.8	9.8	8.1 – 11.7
Metal oxides	10.1	6.3 – 15.2	6.0	4.6 – 7.6
Silicates + sea-salt	32.8	26.3 – 39.8	63.8	60.9 – 66.7
Sulfates	5.1	2.4 – 9.1	6.2	4.8 – 7.8
Secondary	4.0	1.8 – 7.8	1.4	0.8 – 2.3
Droplets	9.1	5.5 – 14.0	4.0	2.9 – 5.4
Other	3.0	1.1 – 6.5	1.0	0.5 – 1.8
LA–MS	(n = 146)		(n = 1663)	
OC/BC	30.1	22.8 – 38.3	34.0	31.7 – 36.3
Pb-bearing	0	0.0 – 2.5	11.0	9.5 – 12.6
Industrial metals	6.8	3.3 – 12.2	2.0	1.4 – 2.8
Minerals + metals	62.3	53.9 – 70.2	42.0	39.6 – 44.4
Other	0.7	0.0 – 3.8	11.0	9.5 – 12.6

Fig S1: Hourly backward-trajectories for period A of Fig. 1 at the Jungfraujoch station. Trajectories were calculated by the offline HYSPLIT4 model (rev. 521) (Draxler and Rolph, 2014), based on GDAS data (available from ftp://gdas-server.iarc.uaf.edu). Vertical wind field was used for calculation vertical movement.

HYSPLIT (HYbrid Single-Particle Lagrangian Integrated Trajectory) Model access via NOAA ARL READY Website: http://www.arl.noaa.gov/HYSPLIT.php, access: Nov 25, 2014, 2014.

NOAA HYSPLIT MODEL

Backward trajectory ending at 1200 UTC 02 Feb **

GDAS Meteorological Data

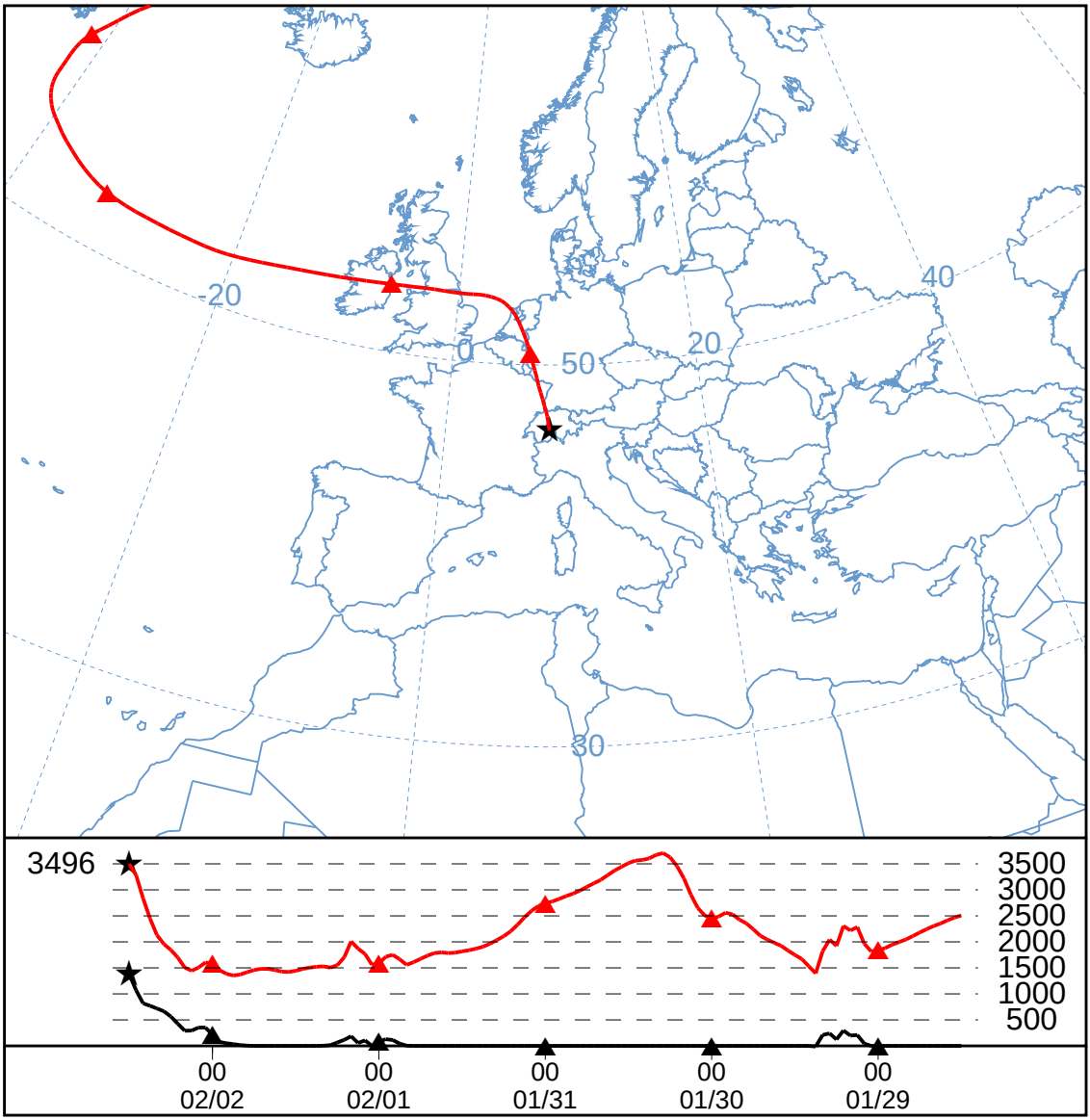

NOAA HYSPLIT MODEL

Backward trajectory ending at 1300 UTC 02 Feb **

GDAS Meteorological Data

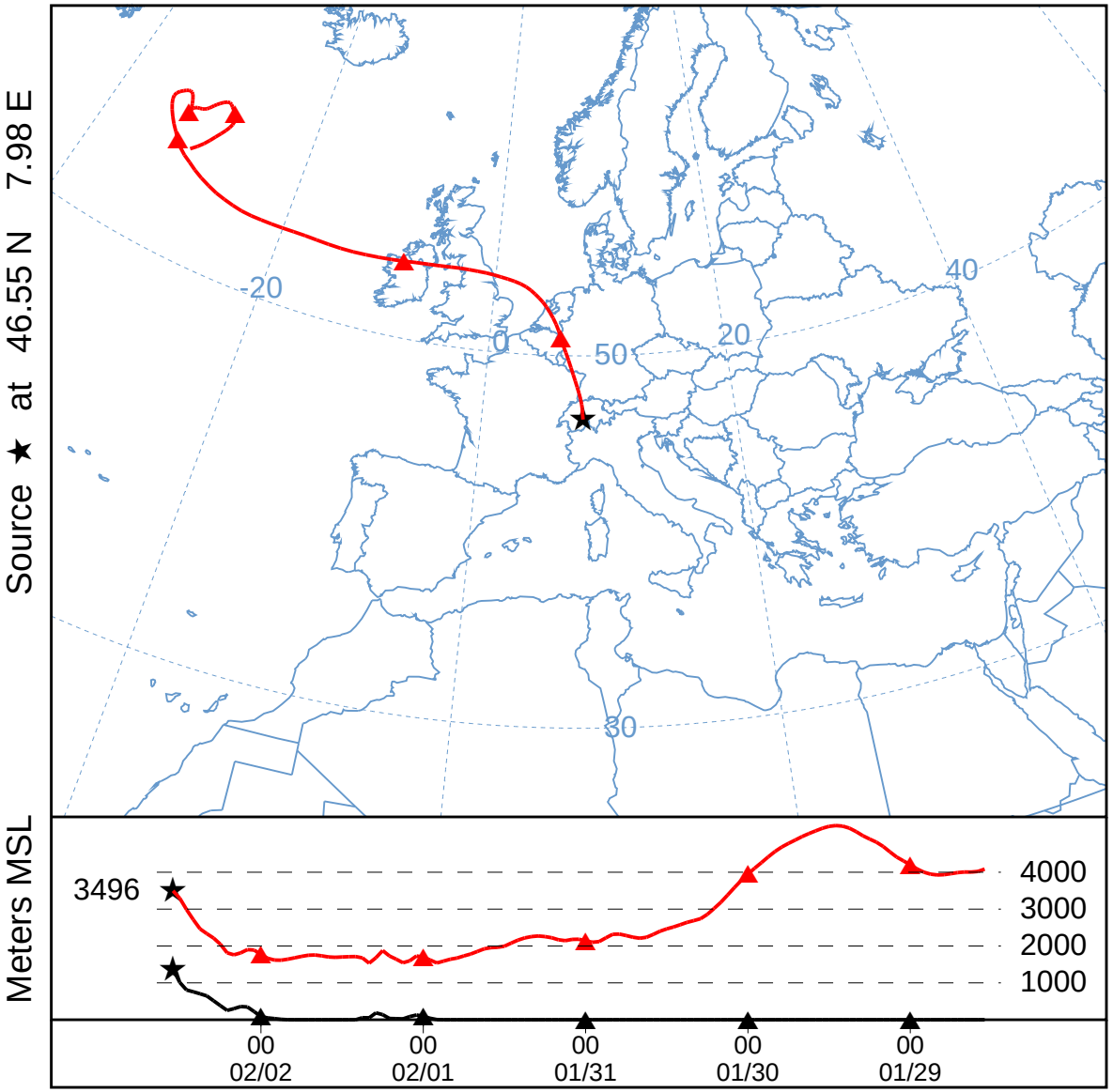

NOAA HYSPLIT MODEL

Backward trajectory ending at 1400 UTC 02 Feb **

GDAS Meteorological Data

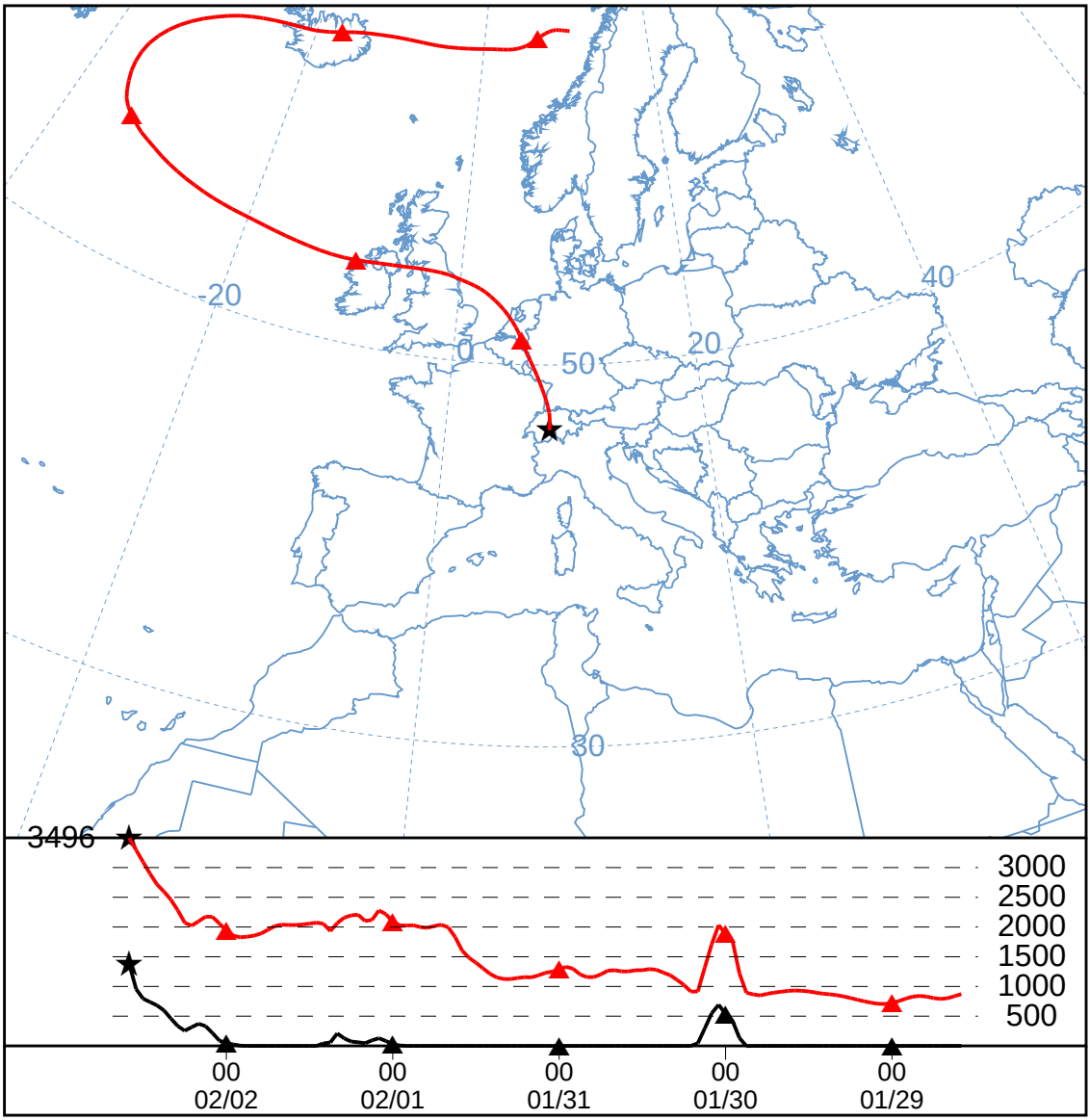

NOAA HYSPLIT MODEL

Backward trajectory ending at 1500 UTC 02 Feb **

GDAS Meteorological Data

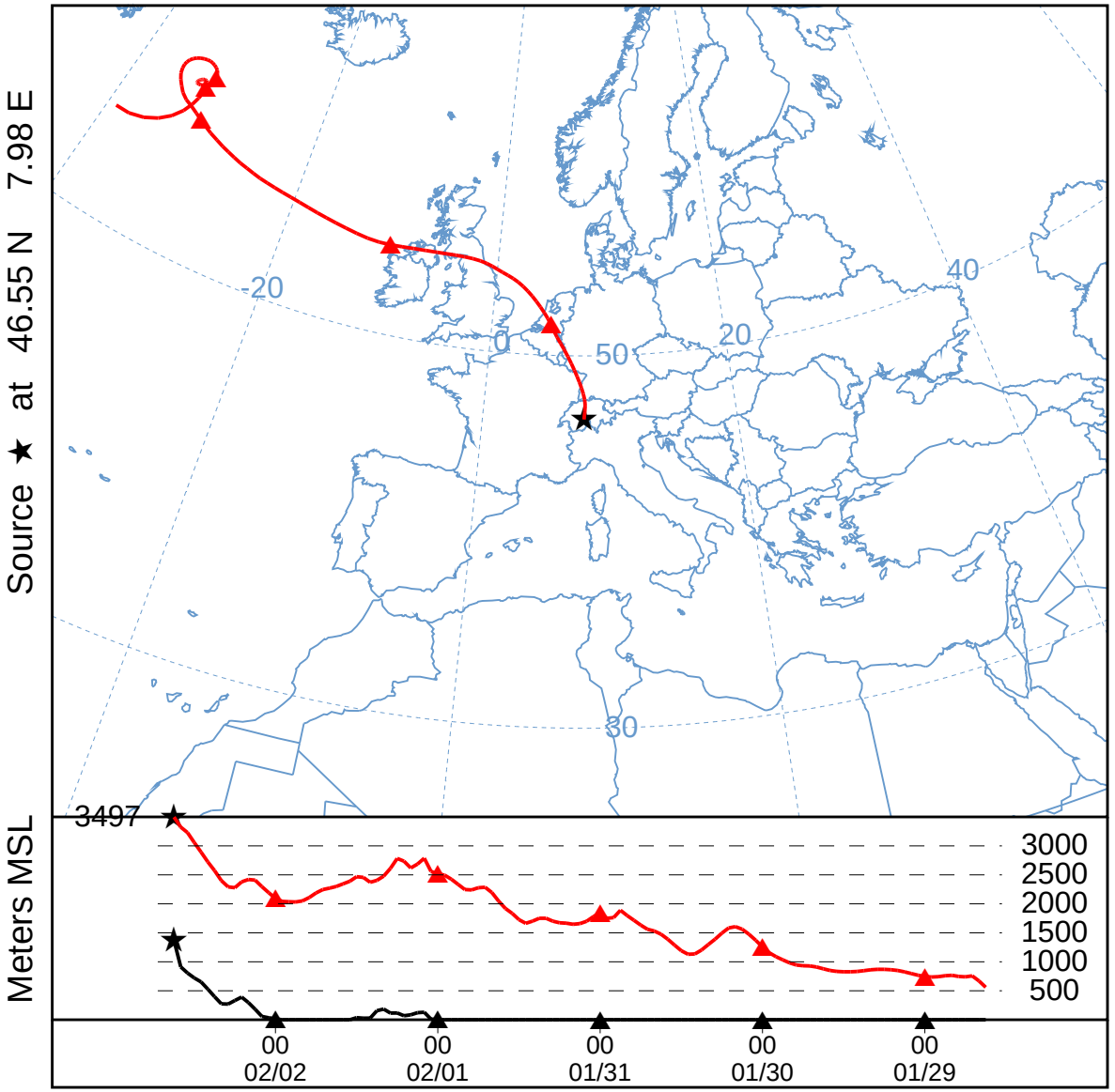

NOAA HYSPLIT MODEL

Backward trajectory ending at 1600 UTC 02 Feb **

GDAS Meteorological Data

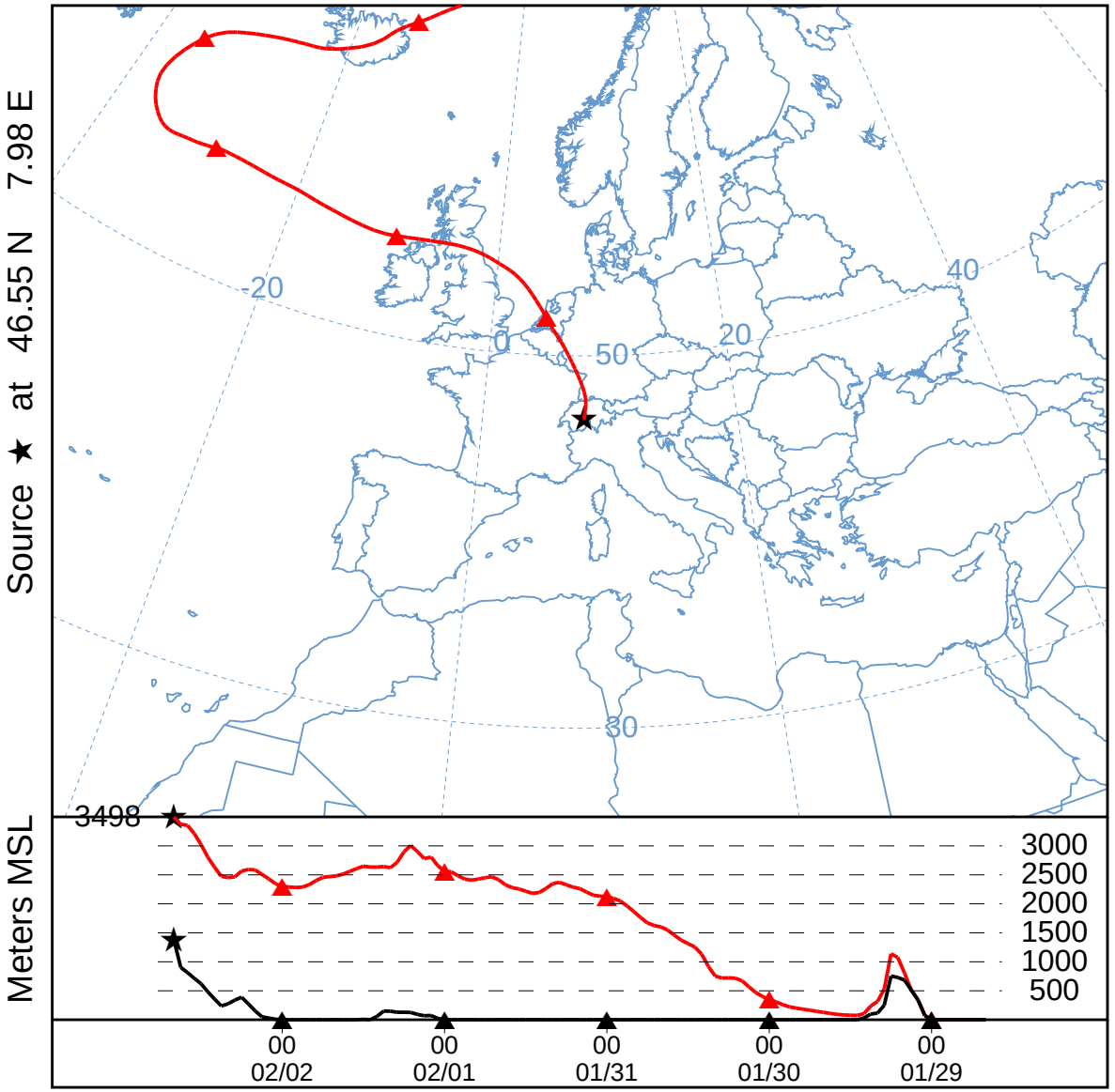

NOAA HYSPLIT MODEL

Backward trajectory ending at 1700 UTC 02 Feb **

GDAS Meteorological Data

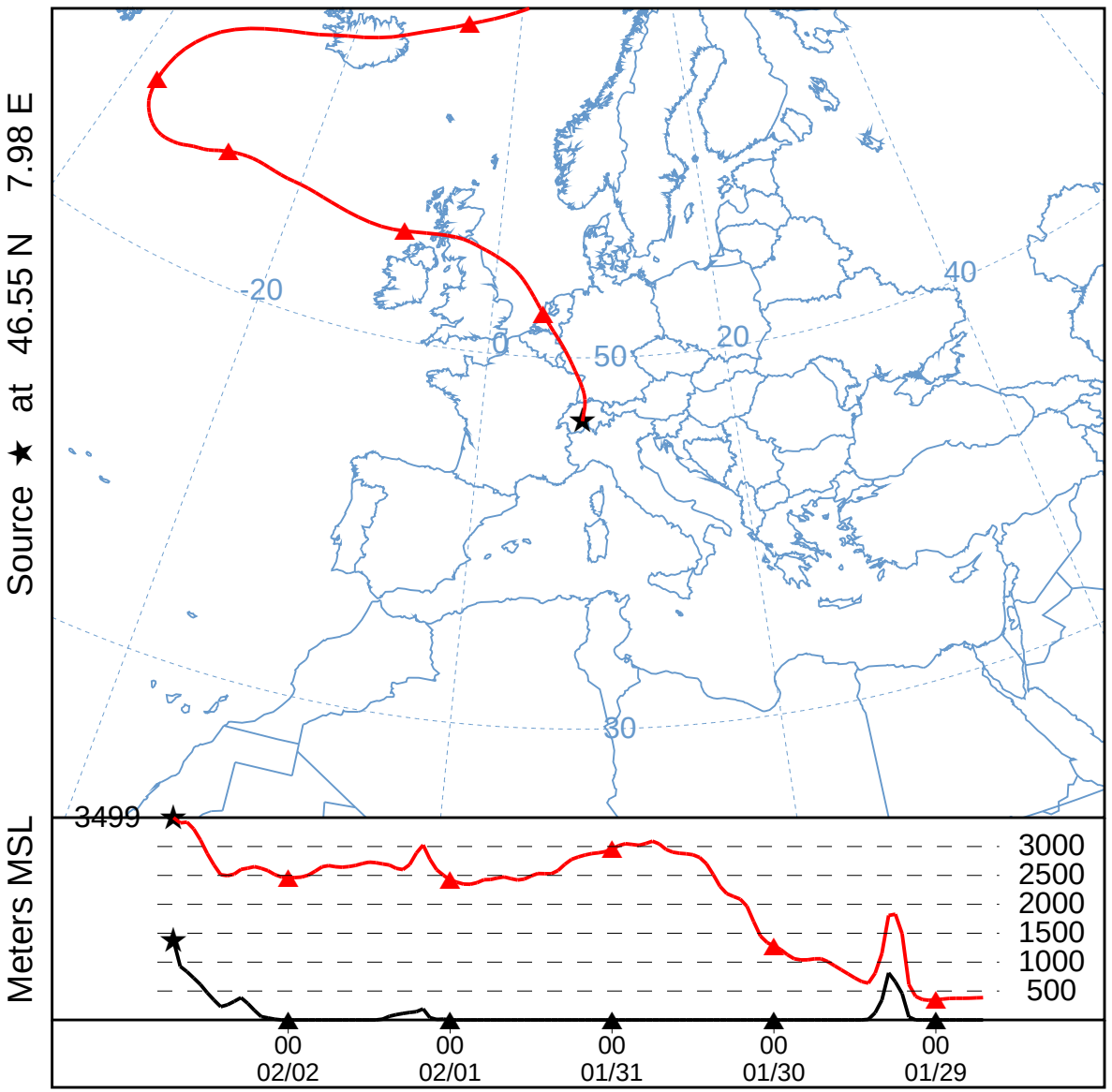

NOAA HYSPLIT MODEL

Backward trajectory ending at 1800 UTC 02 Feb **

GDAS Meteorological Data

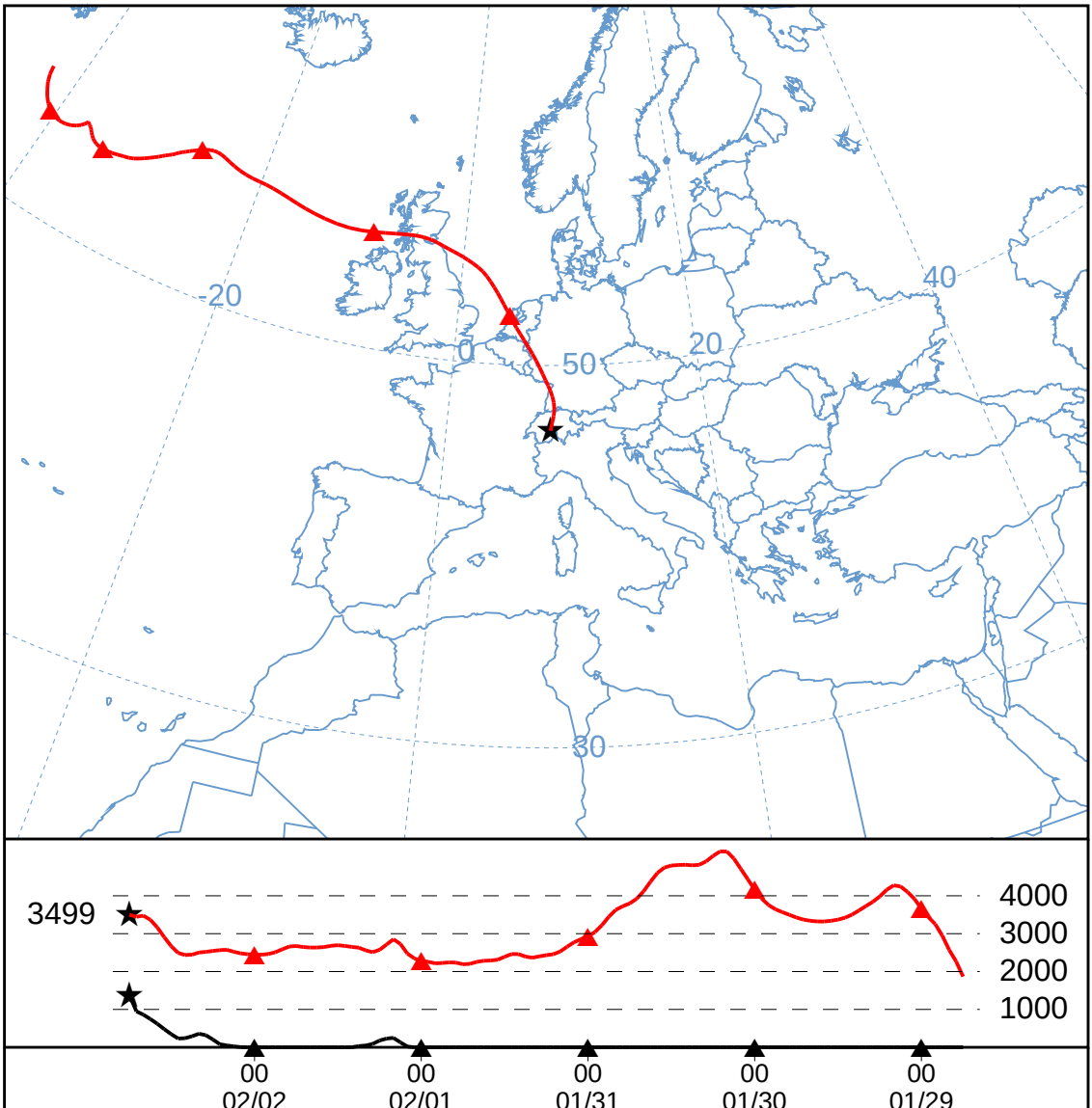

NOAA HYSPLIT MODEL

Backward trajectory ending at 1900 UTC 02 Feb **

GDAS Meteorological Data